SPECTROMETRIC OBSERVATIONS OF JUPITER S–BURSTS AT THE OBSERVATORY LUSTBUEHEL, GRAZ

H. O. Rucker*, V. Mostetschnig*, H. P. Ladreiter*, and G. K. F. Rabl*

Abstract

After the deployment of logarithmic–periodic antennas on the grounds of the Observatory Lustbuehel, spectrometric observations have been performed for Jovian millisecond radio burst investigation. The linear polarized antennas are capable for reception of radio waves in the frequency range of 13 MHz $\leq$ f $\leq$ 30 MHz. Within the frequency interval of 20 MHz $\leq$ f $\leq$ 30 MHz the multichannel radio receiver is able to simultaneously observe 50 frequencies with a respective bandwidth of 20 kHz, thus a 1 MHz spectrometry, arbitrarily placed within the antenna frequency range, can be done with a time resolution of, at present, 2 milliseconds.

Examples of S–burst dynamic spectra will be discussed, in particular obtained during the Io–B storm on February 20, 1991, within the frequency range of 26 MHz – 27 MHz.

1 Introduction

At the Observatory Lustbuehel, located in the Eastern outskirts of Graz, a Jupiter radio station has been monitoring the Jovian decameter radio emission since 1987. These first measurements had been interferometric observations at two fixed frequencies, using two antennas along an East–West–baseline of 80 m [Rucker and Mostetschnig, 1988].

After the deployment of logarithmic–periodic antennas at the end of 1989, a multichannel radio receiver was brought into operation. This 50–channel receiver enables the simultaneous measurement of 50 adjacent frequencies, each with a bandwidth of 20 kHz. Thus a complete coverage of 1 MHz can be obtained. This 1 MHz observational coverage can arbitrarily be placed within the possible antenna–receiver frequency window, between 20 MHz and 30 MHz. Section 2 gives a short description of the present configuration of the Jupiter radio station, with some more details on digitizing, data storage, and data display.

Section 3 deals with observations, in particular with the S–burst event from February 20, 1991. In the subsequent chapter some specific spectra are analyzed, with special

*Space Research Institute, Austrian Academy of Sciences, Halbärthgasse 1, 8010 Graz, Austria

emphasis on the inherent Faraday effect in the spectra and possible implications for remote sensing. The final section 5 describes future activities and planned investigations within the framework of international cooperations.

2 The multichannel spectrometer

The multichannel receiver has the capability of receiving frequencies in the range of 20 MHz $\leq$ f $\leq$ 100 MHz, but the log–per antennas are adjusted only for the frequency interval 13 MHz $\leq$ f $\leq$ 30 MHz reasonable for ground–based observation of Jovian decameter radio emission.

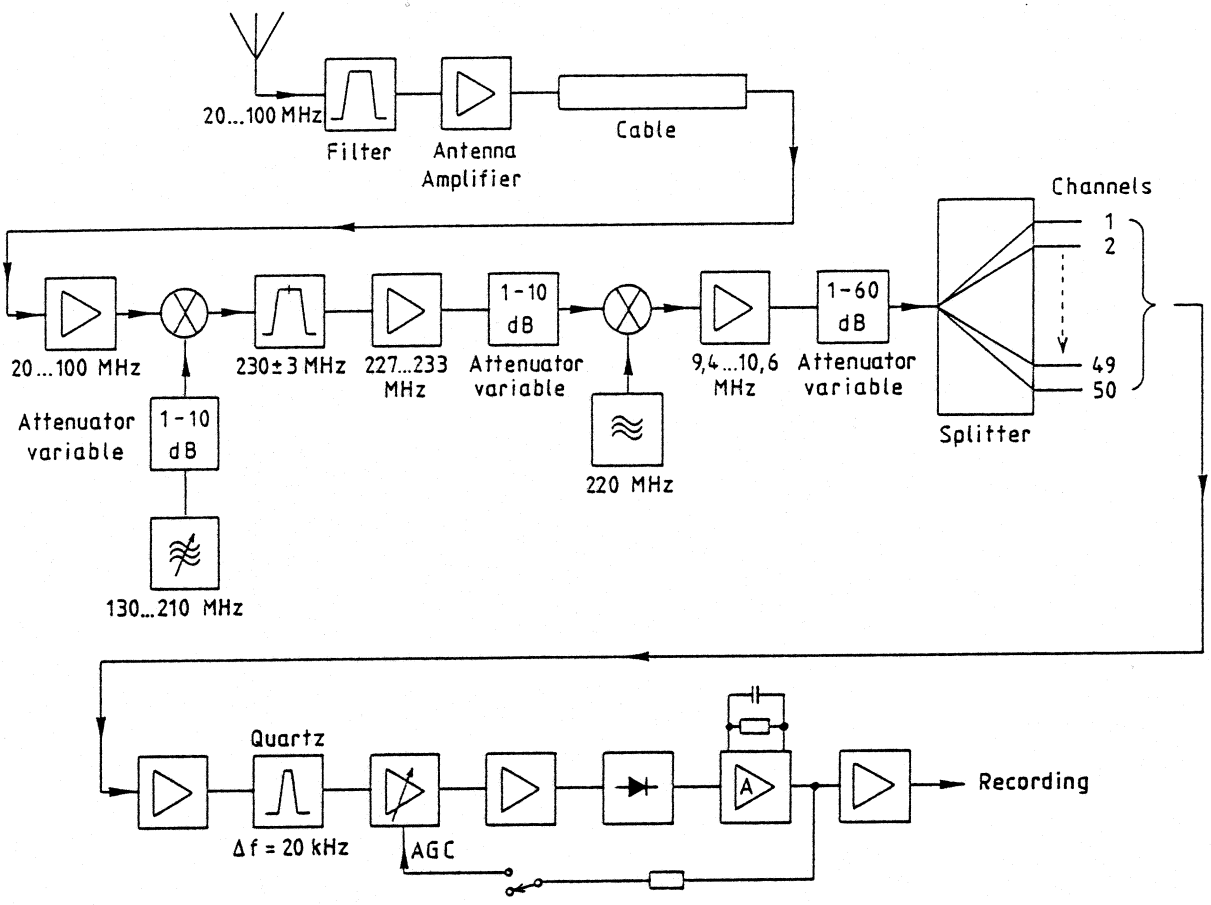

Figure 1: Flow diagram of the 50–channel receiver for spectrometric observation of the Jupiter DAM radio emission.

The general structure of the multichannel receiver is shown in Figure 1. Within the filter bandwidth the signals get enhanced by a broadband amplifier immediatedly after the antenna in order to cope with the cable losses between the antenna and the receiver. An additional amplifier at the receiver inputs yields further signal voltage increase, but the essential importance of this amplifier is to better adapt the 50Ω–antenna cables to the first mixer. Transformation is performed by a precise and amplitude constant, variable

oscillator. A variable attenuator (between 1 and 10 dB) works as decoupling and adapting stage.

The mixed signal passes a relatively narrow bandpass filter with a center frequency of 230 MHz and 6 MHz bandwidth. Over a further variable attenuator the first intermediate frequency controls the second mixer. By heterodyning of 220 MHz a difference frequency of 10 MHz is generated. A subsequent bandpass filter provides a receiving bandwidth of about 1 MHz, which – by means of the first local oscillator – can arbitrarily be placed within the reception frequency interval.

Now the 1 MHz bandwidth gets a spectral separation by 50 individual channels with each 20 kHz bandwidth. The main components are 50 quartz filters which completely cover the frequency interval between 9.5 MHz and 10.5 MHz. In order to perform a controlled separation a power splitter separates this second intermediate frequency into 50 branches. The adjacent attenuator, variable over a wide range, enables an adaptation to different intensities at various frequencies.

The structure of all 50 individual frequency channels is identical, so the general diagram of but one receiving channel is shown in Figure 1 (bottom). After a preamplifier a quartz filter is placed with a filter opening of $\Delta f = 20$ kHz (e.g. 9.50 MHz $\leq f \leq$ 9.52 MHz). Subsequently a 2 step channel amplifier - with variable first step - follows. The high frequency signal, in the ideal case modulated by radio noise, is guided to the demodulation diode, where a separation of high and low frequency takes place. An active low pass filter with variable time constant smoothes the signal. The low frequency voltage as regulating voltage can, on the one side, be directed back to the variable amplifier, on the other side it is guided into the recording unit.

3 The recording unit

At a certain instant of time the receiver provides 50 voltage values (integrating time constant approximately a tenth of a millisecond), corresponding to the actual level of reception. These voltage values and some other additional information regarding time and frequency are sequentially guided over an analog multiplexer (Figure 2). The sampling procedure is performed with a frequency of 32768 Hz; the sampling of the 50 receiver channels and additional 14 channels for time information, color code and grid of the spectrum needs about 2 ms. Within half a second 256 sampling cycles are performed. An 8 bit analog–digital–converter (ADC) synchronously digitizes the voltage values (which change by 30.5 microseconds) and guides the data to the alternating storage system, consisting of 2 random access memories (RAMs). Each RAM can store data for half a second, i.e. 16384 bytes. Obviously, the storage is done with an alternating scheme: During write–in of RAM 1 the other RAM 2 will be read–out, and vice–versa.

Now the stored data are displayed on a monitor in such a way that a dynamic spectrum is generated by the 50 receiver channels (Figure 3). Frequency (vertical axis) covers 1 MHz and time (horizontal axis) shows half a second. The above mentioned frequency and time resolution yields a pixel of 20 kHz versus 2 ms. As can be seen in Figures 4, 5, 8, and

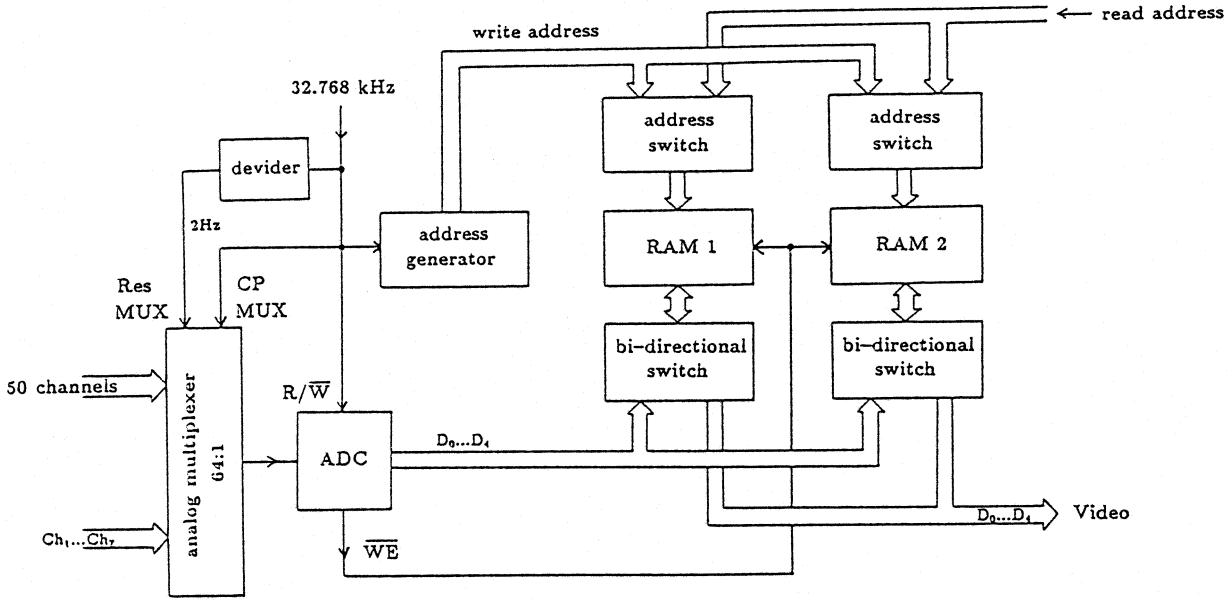

Figure 2: Block diagram of the digitizing and data storage. (Res = reset, MUX = multiplexer, CP = clock pulse, $R/\overline{W}$ = read/write signal, $\overline{WE}$ = control signal for RAM writing process, $D_0...D_4$ = data line).

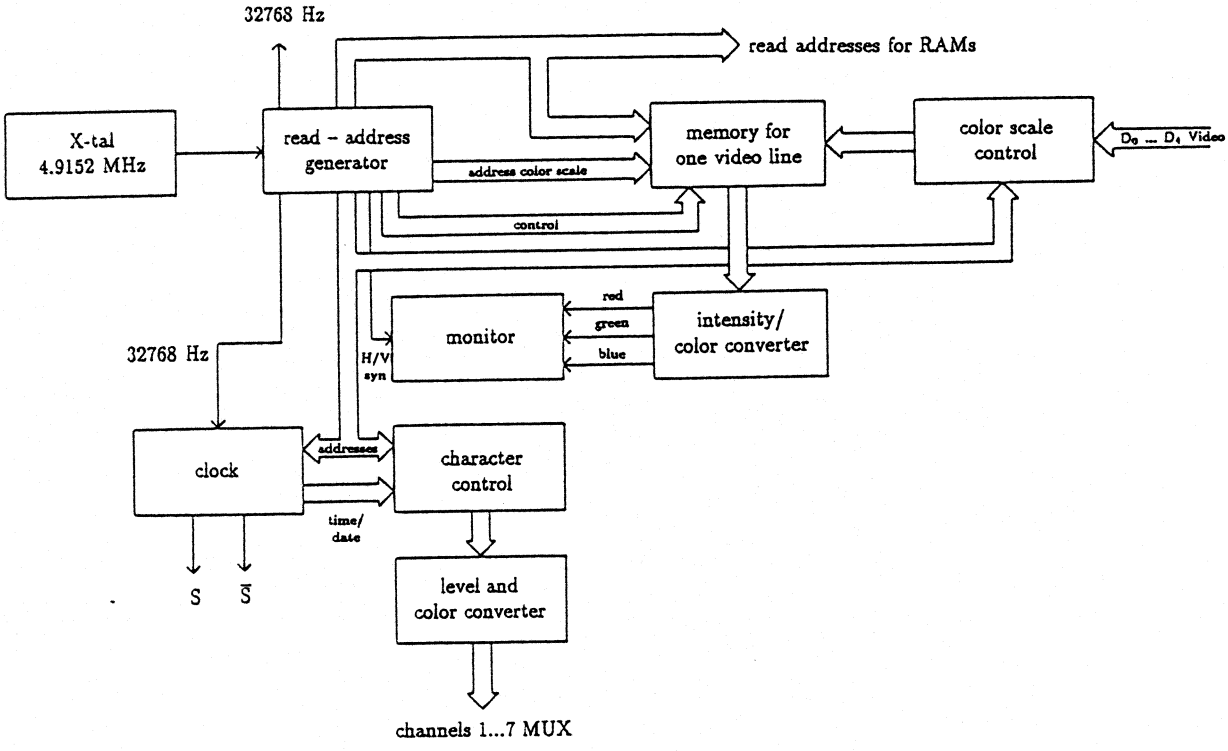

Figure 3: Schematics of the monitor control. (H/V syn = Horizontal/Vertical synchronization; S, $\overline{S}$ = signals for camera control).

9, on top of each spectrum an information panel displays mean frequency (MHz), date (year and day of year), Jupiter symbol, and time (hours, minutes, seconds). The essential dynamic spectrum is bordered by a color code strip, which displays 32 different colors. The intensity limit to the left, displayed at dark blue, equals −115 dBm. The level of intensity is increasing to the right, up to −65 dBm, thus ranging over 50 dB.

Since the data sequence within 2 milliseconds is originally generated and stored by increasing frequency, but the monitor screen can only be fed by lines, a data address transformation is necessary in order to enable a read–out by channels onto the screen. Each channel line on the screen consists of 6 information lines (carrying the same spectral information) and 2 dark lines. The transformation of the various intensity levels into 32 different colors is done by a programmed memory (PROM).

At present, the monitor display cannot digitally be stored. Thus, the recording unit is completed by a movie camera which, in the mode of single frame shots, stores each half second dynamic spectrum on film. With a 60 m film roll almost 7900 pictures can be taken which enables more than one hour registration of half second spectra.

The S–burst event of February 20, 1991

Out of a number of Io–B events during the observation campaign 1990/91 some S–burst events could be observed. One particular event, outstanding by the intensity and variety of the observed S–bursts, was the Io–B radio storm from February 20, 1991. Within the observed frequency range of 26 MHz $\leq$ f $\leq$ 27 MHz strong S–burst activity was recorded between 22:40 UT and 23:23 UT. The corresponding coordinates within the CML–Io phase diagram are CML = 137.1° and γ_{Io} = 84.3° for the onset and CML = 163.1° and γ_{Io} = 90.4° for the end of the observed S–burst activity.

First evidence of S–burst activity sporadically occurred in the structure of narrow single bursts with a constant frequency duration (CFD) of a few milliseconds (not exceeding 10 ms). Within the frequency range of Δf = 1 MHz the life time is also very short, approximately 30 ms, which results in a relatively high drift rate of about −30 MHz/s. This pattern continues for a couple of minutes. Then an S–burst train shows up, containing bursts with a sometimes high burst repitition rate.

The further development exhibits millisecond bursts with increasing CFD, also new features show up: Arc–structured bursts with a flaring at the low frequency end (Figure 4). These spectra provide clear evidence of the inherent Faraday effect (see subsequent section). The observed burst intensity is significantly increasing. Specific parts within the burst structure show a ‘deep yellow’ color. Applying the color code on the spectra the bursts have intensities which correspond to approximately 30 dB above the least detectable burst intensity of −115 dBm.

The S–burst features now turn into ‘patchy’ structures, the almost horizontally ordered intensity maxima and minima generated by the Faraday effect are clearly visible (Figure 5).

A further characteristic which can be seen in the spectra is the slowly drift in frequency of the band of S–burst activity, appearing at the upper frequency limit (f = 27 MHz) and approaching the lower frequency limit (f = 26 MHz) within several tens of seconds. This S–burst 'band' drift towards lower frequencies is often observed (see e.g. Aubier et al., [1988], Figure 1). A comparison of data obtained by the Nançay radio station during the same period of time of this particular Io–B event confirmed these findings [P. Zarka and A. Lecacheux, private communication]. As could be seen by the Nançay wide frequency recordings new S–burst activity started at about 28 MHz and moved down into our frequency window.

After some high intensity bursts with rather patchy structures the final episode of this Io–B S–burst event fades out with single bursts of low intensity and small frequency range.

Out of several parameters which characterize the appearance of a single S–burst, the burst drift rate df/dt is a rather valuable parameter. S–bursts always have negative drift, which is dependent on frequency [Leblanc et al., 1980] and the Jovian declination of the observer [Riihimaa, 1978; 1979]. The analysis of the present S–burst event with regard to frequency drift yielded rather high drift values. Subsets of continuous S–burst observation (duration generally 10 seconds) were analyzed to determine df/dt. Figure 6 shows that the drift rates for each subset are around −30 MHz/s, which is, considering the observation mean frequency of f = 26.5 MHz, a few MHz/s off the drift values found by several other investigations [Leblanc et al., 1980; Figure 3]. A study from Ellis shows histograms of the magnitude of df/dt for different wave frequencies [Ellis, 1982; Figure 7], which provide a small probability for drift rates around −30 MHz/s for an S–burst frequency of f = 27 MHz.

In order to get an impression of the diversity of S–burst features which occur within a few seconds, Figure 7 summarizes three seconds of recordings starting from t=22:45:27.5 UT. As can be seen from the dynamic spectra the S–bursts exhibit a wide range of different features. The constant frequency duration varies from a few milliseconds up to several tens of milliseconds. A further characteristic is visible in the spectra: Within the burst structures some bright spots indicate intensity enhancements at certain frequencies. In the sequence of dynamic spectra of Figure 7 these intensity enhancements appear at distinct frequencies throughout the whole series of spectra. This phenomenon is due to the Faraday effect as described below in detail.

Figure 4: (color plot, next page, top) Dynamic spectrum of S–bursts during the Io–B radio storm of February 20, 1991. Time is 23:44:51.0 (hours:minutes:seconds Mediterranean Time, corresponding to UT plus 1 hour). Mean frequency is f = 26.5 MHz with a frequency range of +/– 500 kHz, with frequency increasing from top to bottom. The spectrum exhibits a frequency resolution of 20 kHz and a time resolution of 2 milliseconds. A characteristic arc–shaped S–burst shows 'flaring' at the low frequency end.

Figure 5: (color plot, next page, bottom) Dynamic spectrum obtained at 22:44:51.5 UT (half a second later with regard to Figure 4). With dependence of frequency an alternating intensity pattern is visible within the S–burst structure.

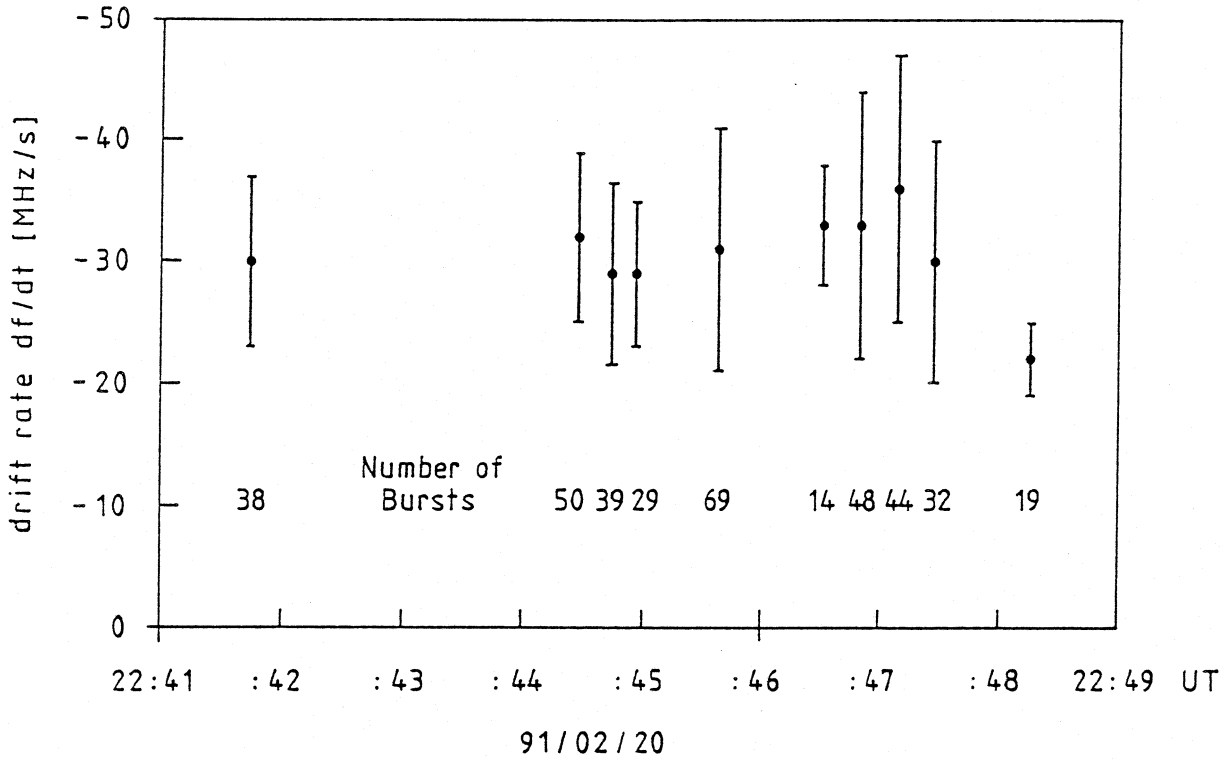

Figure 6: Frequency drift measured during subsets of the Io–B S–burst storm on February 20, 1991, at f = 26.5 MHz mid frequency. The drift rates are mean values (the vertical bars indicate one standard deviation) within 10 seconds. (The period with 69 bursts comprises 22 seconds.)

4 The Faraday effect in the spectra

A significant number of dynamic spectra of the above described S–burst event gives evidence of an inherent Faraday effect. Intense burst structures show horizontal intensity maxima and minima. Since the Jovian decametric emission is predominantly right–hand elliptically polarized [Boudjada and Lecacheux, 1991], the E-vector of the wave suffers Faraday rotation which is due to the phase difference of the extraordinary and ordinary modes when propagating through a birefringent medium. This results in the well-known Faraday fringes which modulate the dynamic spectrum of the emission when it is observed with a linear polarized antenna.

By means of the intensity code strip bordering the dynamic spectra at top and bottom an intensity level above detection threshold can be defined. Since the intensity level corresponding to darkest blue equals −115 dBm and since 32 intensity steps cover 50 dB, we are able to determine qualitatively the relative intensity differences between apparent intensity maxima and minima due to the Faraday effect.

It is most important to determine the ellipticity of the polarisation ellipse of the S–bursts like those shown in Figure 8, e.g. We recognize that the intensity ratio between the intensity maxima (yellow color) and the minima (green–blue color) is some 17 dB. By the assumption of the intensity maxima occurring when the major axis a of the polarization ellipse is parallel to the antenna element and the minima occurring when the minor axis b

is parallel to the element the axial ratio is $a/b = -\sqrt{10^{1.7}}$. (The negative sign represents extraordinary wave mode.) The degree of circular polarization d_c and the degree of linear polarization d_l are then given by

$$d_c = \frac{2\frac{a}{b}}{\frac{a^2}{b^2} + 1} \tag{4.1}$$

$$d_l = \frac{\frac{a^2}{b^2} - 1}{\frac{a^2}{b^2} + 1} \tag{4.2}$$

The values of d_c and d_l are -0.28 and 0.96, respectively, and are qualitatively consistent (although the value d_c is somewhat lower in this study) with the results of Lecacheux et al. [1991] who analyzed Io–B storms recorded at the Nançay radio observatory in France.

The Faraday effect can be used as a tool for remote sensing the electron content in the terrestrial ionosphere and the Jovian magnetosphere, since the amount of Faraday rotation for a given frequency and the respective spacing (in frequency) of Faraday fringes visible on the dynamic spectrum is dependent on the physical properties (plasma density, magnetic field) of the medium through which the emission must propagate to reach the observer. In a first approximation the rotation angle of the E–vector is proportional to $1/f^2$ [Leitinger, this issue]. Of course, this $1/f^2$ frequency dependence cannot be seen in a 1MHz frame, but the 'fringe spacing', the frequency range between two maxima (or minima) can be determined.

In the dynamic spectrum of Figure 8 the fringe spacing is approximetely $\Delta f \approx 140 - 160$ kHz. A comparison with Io–B radio burst measurements obtained from other stations (Nançay, France; Gainesville, USA) shows that the fringe spacing can vary, due to varying plasma parameters (electron content, magnetic field) along the ray path, from less than 100 kHz up to several hundreds of kHz [Phillips et al., 1989].

Figure 7: (color plot, next page) Dynamic spectra obtained during three consecutive seconds, starting at t = 22:45:27.5 UT. As can be seen in the spectra, the S–bursts exhibit a wide range of constant frequency duration, from a few milliseconds up to several tens of milliseconds.

Figure 8: (color plot, following page, top) Clear evidence of the inherent Faraday effect is visible in this spectrum obtained at t = 22:45:38.0 UT.

Figure 9: (color plot, following page, bottom) Intensity maxima have shifted in frequency, with regard to Figure 8, by half the fringe spacing.

The measurement of the Faraday effect over a wide frequency range enables the determination of the total and absolute number of Faraday rotation of a linear polarized wave between the source location and the terrestrial point of observation [Boudjada and Lecacheux, 1991]. This may finally serve as a tool for remote sensing the terrestrial and Jovian magnetospheres.

The limited frequency range of 1 MHz, of course, does not allow any detailed studies as explained above. But, as found from Figures 8 and 9, a change in the frequency dependent location of the intensity maxima gives some clue to possible terrestrial ionospheric variations. The dynamic spectrum of Figure 9 displays intensity maxima, which are shifted in frequency with regard to Figure 8 (seven minutes earlier), by half the fringe spacing. With the assumption of predominant terrestrial electron density variation the 'fringe shifting' of half a half rotation corresponds to a variation of ΔN of the total electron content (TEC) of approximately 0.6% within about seven minutes [Leitinger, private communication].

5 Aspects of future investigations

Since both time and frequency resolution as well as data display of the S–burst dynamic spectra are to a certain extent comparable to other established stations, e.g. Nançay (France), Oulu (Finland), Gainesville (Florida, USA), the most urgent improvement obviously has to be done in the extension of the multichannel frequency range. There exist already detailed studies with regard to a frequency range extension of up to 4 MHz, also arbitrarily be placed within the antenna–receiver frequency window. The essential point will be keeping the time resolution of at present 2 milliseconds.

An additional supplement will be the deployment of a parallel radio receiver scanning a wide frequency range for detecting Jovian DAM activity in order to place the multichannel receiver into the right frequency regime. This can be done by a spectrum analyzer where the data – with low time resolution – are in real time displayed on a monitor. Corresponding experimental studies are in progress.

In close connection with these experimental improvements, theoretical studies should investigate the millisecond burst generation mechanism and the propagation of these bursts through the magnetoplasma of the Jovian magnetosphere, the interplanetary medium, and the terrestrial magnetoplasma.

One future aspect would be the establishment of an international network comprising European Jupiter radio stations in order to perform simultaneous S–burst measurements. So far respective observations have only be performed and analyzed by single stations. Considering the local terrestrial ionospheric conditions an improved 'remote sensing' of the Jovian magnetosphere – along the ray path – , in particular of the radio source regions, could possibly be obtained.

Acknowledgements: The authors are grateful to the Observatoire de Paris–Meudon, Groupe Decametrique, in particular to Yolande Leblanc and Alain Lecacheux, for having provided the 50–channel receiver from Nançay (France) which is now, after some repair and modification, the central element of the S–burst spectrometry at the Observatory Lustbuehel Jupiter radio station.

References

Aubier, M. G., W. Calvert, and F. Genova, Source localization of Jupiter's Io dependent radio emissions, in *Planetary Radio Emission II*, edited by H. O. Rucker, S. J. Bauer, and B. M. Pedersen, p. 113, Austrian Academy of Sciences Press, Vienna, 1988.

Boudjada, M. Y., and A. Lecacheux, Faraday rotation of Jupiter's decametric radiation, *Astron. Astrophys.*, **247**, 235, 1991.

Ellis, G. R. A., Observations of the Jupiter S–bursts between 3.2 and 32 MHz, *Austral. J. Phys.*, **35**, 165, 1982.

Leblanc, Y., M. G. Aubier, C. Rosolen, F. Genova, and J. de la Noe, The Jovian S–bursts: II. Frequency drift measurements at different frequencies throughout several storms, *Astron. Astrophys.*, **86**, 349, 1980.

Lecacheux, A., A. Boischot, M. Y. Boudjada, and G. A. Dulk, Spectra and complete polarization state of two, Io–related, radio storms from Jupiter, *Astron. Astrophys.*, **251**, 339, 1191.

Leitinger, R., Propagation effects influencing the observations of planetary radio emissions, this issue.

Phillips, J. A., T. C. Ferree, and J. Wang, Earth–based observations of Faraday rotation in radio bursts from Jupiter, *J. Geophys. Res.*, **94**, 5457, 1989.

Riihimaa, J. J., Drift rates of Jovian S–bursts, *Astron. Astrophys.*, **63**, L27–L28, 1978.

Riihimaa, J. J., Drift rates of Jupiter's S–bursts, *Nature*, **279**, 783, 1979.

Rucker, H. O., and V. Mostetschnig, Interferometric observations at 16.7 and 22.2 MHz at the Observatory Lustbuehel, Graz, in *Planetary Radio Emissions II*, edited by H. O. Rucker, S. J. Bauer, and B. M. Pedersen, p. 87, Austrian Academy of Sciences Press, Vienna, 1988.